

Avalanches in 2D Dislocation Systems: Plastic Yielding is not Depinning

Péter Dusán Ispánovity¹, Lasse Laurson², Michael Zaiser³, István Groma¹, Stefano Zapperi^{4,5}, and Mikko J. Alava²

¹*Department of Materials Physics, Eötvös University Budapest, H-1517 Budapest, POB 32, Hungary*

²*COMP Centre of Excellence, Department of Applied Physics, Aalto University, P.O. Box 14100, FIN-00076 Aalto, Espoo, Finland*

³*Institute of Materials Simulation, Department of Materials Science, University of Erlangen-Nürnberg, Dr.-Mack-Str. 77, 91062 Fürth, Germany*

⁴*CNR-IENI, Via R. Cozzi 53, 20125 Milano, Italy and*

⁵*ISI Foundation, Via Alassio 11/C, 10126 Torino, Italy*

We study the properties of strain bursts (dislocation avalanches) occurring in two-dimensional discrete dislocation dynamics models under quasistatic stress-controlled loading. Contrary to previous suggestions, the avalanche statistics differs fundamentally from predictions obtained for the depinning of elastic manifolds in quenched random media. Instead, we find an exponent $\tau = 1$ of the power-law distribution of slip or released energy, with a cut-off that increases exponentially with the applied stress and diverges with system size at all stresses. These observations demonstrate that the avalanche dynamics of 2D dislocation systems is scale-free at every applied stress and, therefore, can not be envisaged in terms of critical behavior associated with a depinning transition.

PACS numbers: 81.40.Lm, 61.72.Lk, 68.35.Rh, 81.05.Kf

Crystalline solids subject to an increasing stress undergo a transition (“yielding”) from nearly-elastic behavior to plastic flow by collective dislocation motion. Both during the run-up to yielding and in the subsequent plastic flow regime, dislocation systems exhibit strongly intermittent, avalanche-like dynamics. In micron sized specimens these avalanches show as abrupt strain bursts with a broad, power law-type size distribution [1, 2] (for a review see [3]) and in larger samples they manifest themselves through acoustic emission (AE) events with power-law distributed amplitudes [4, 5].

Several researchers have advanced the idea that the dislocations in a crystal deforming under stress might be envisaged as a driven non-equilibrium system, where power-law distributed avalanches arise from dynamic critical behavior associated with a non-equilibrium phase transition at a critical value $\sigma_{\text{ext}} = \sigma_c$ of the externally applied stress, analogous to the depinning transition of elastic interfaces in random media [6]. This idea applies in a straightforward manner to single dislocations interacting with immobile impurities which provide a textbook example of one-dimensional elastic manifolds undergoing a depinning transition [7, 8]. In generalization of this observation, several authors have argued that the mean-field limit of the depinning transition might correctly describe the dynamic behavior of stress-driven many-dislocation systems even when other defects (such as impurities) are absent [9–14]. In this picture plastic yielding is envisaged as a continuous phase transition where the external stress acts as control parameter and a critical point is reached at the yield stress. There are several motivations for such an analogy: (i) dislocation-dislocation interactions are of long-range nature, implying that a mean-field description could be applicable, and (ii) the strain burst distribution appears to be a power law, $P(\Delta\gamma) \propto \Delta\gamma^{-\tau}$, with τ found to be $\tau \approx 1.5$ both

experimentally and numerically [1, 2, 15–17], in apparent agreement with mean-field depinning (MFD) [6].

There are, however, several unresolved issues regarding the validity of the depinning picture. In the classical depinning scenario, an elastic manifold interacts with a *static* (quenched) pinning field representing immobile impurities of the medium. However, yielding and avalanche dynamics of plastic flow are generic features of crystal plasticity which do not require impurities or other types of quenched disorder. Discrete dislocation dynamics (DDD) models [18–22, 24], which are commonly used to model plasticity of pure fcc crystals, relate the yield stress to the mutual trapping (or *jamming* [22, 23]) which occurs as interacting dislocations form complex metastable structures even in the absence of other defects [2, 5, 22, 25]. This important difference is illustrated schematically in Fig. 1.

Even if we consider the dynamics of the simplest possible DDD model – a $2d$ system of straight parallel dislocations moving on a single slip system – there are several findings which are not consistent with MFD. These include: (i) For the relaxation exponent of the Andrade creep law, i.e., the initial power law decay of the mean strain rate under constant applied stress, $\langle \dot{\gamma}(t) \rangle \propto t^{-\theta}$, one finds the value $\theta \approx 2/3$ [22, 26] whereas MFD predicts $\theta = 1$ for the critical relaxation of the order parameter [6, 28]. Also the temporal scaling of the spatial fluctuations of the local creep rates indicates non-mean field behaviour [27]. Moreover, the duration of the power law relaxation regime is at low stresses limited by the system size rather than by the distance $\sigma_{\text{ext}} - \sigma_c$ from the critical point [26], again inconsistent with interface depinning. (ii) The stress-dependence of the steady state strain rate obeys $\langle \dot{\gamma} \rangle \propto (\sigma_{\text{ext}} - \sigma_c)^\beta$, with $\beta \approx 1.8$ [22], while MFD predicts $\beta = 1$ [6]. (iii) The response of the $2d$ DDD model to cyclic applied stresses is not consistent

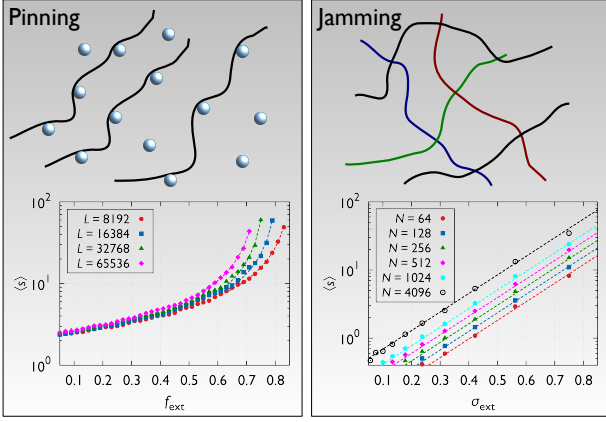


FIG. 1. (color online) Differences between pinning and the present jamming/unjamming scenario. Pinning is induced by quenched disorder which stops the motion of driven elastic manifolds for applied forces f_{ext} below a critical value f_c (top left). With f_{ext} approaching f_c from below, the manifold moves ahead in avalanches with an average avalanche size $\langle s \rangle$ which in MFD diverges as $\langle s \rangle \propto (f_c(L) - f_{\text{ext}})^{-1}$ ($1d$ elastic manifold with elastic interactions decaying as $1/r$, bottom left). f_c depends on the system size L due to finite size scaling, $f_c(L) = f_c(\infty) + aL^{-1}$. In a dislocation system without quenched disorder, dislocation motion may stop due to formation of various jammed dislocation configurations (top right). The behavior of $\langle s \rangle$ we observe in this case is fundamentally different from the depinning scenario, with $\langle s \rangle = A(N)e^{\sigma_{\text{ext}}/\sigma_0}$, where the prefactor $A(N)$ grows with the number of dislocations N (bottom right).

with MFD [29].

Finally, we note that comparisons between theoretical and experimental values of avalanche exponents might be misleading, since most studies of dislocation avalanche statistics consider aggregate distributions (integrated over the different σ_{ext} -values), whereas the theoretical MFD prediction $\tau = 1.5$ refers to stress-resolved distributions. It is known that averaging the distributions over σ_{ext} yields an exponent which is larger than the one of stress-resolved distributions [30], so the numerical and experimental findings of $\tau \approx 1.5$ by themselves do not provide strong evidence for the MFD scenario.

In this Letter, we report results of quasistatic stress-controlled simulations of $2d$ DDD models and demonstrate that the stress-resolved avalanche statistics does not follow the MFD predictions. To underline the general nature of our findings, we consider a continuous time dynamics (CTD) model with continuous spatial resolution and a linear force-velocity relation for the dislocations, together with two spatially discrete cellular automaton (CA) models with different dynamics, finding the same results in all cases.

The DDD models considered here are minimal representations of dislocation systems in deforming crystals,

consisting of straight parallel edge dislocations moving on a single slip system. This implies that the problem reduces to the dynamics of $2d$ systems of point-like objects (the intersection points of the straight parallel dislocation lines with a perpendicular plane) which move on parallel lines in the x direction of a $2d$ Cartesian coordinate system. We consider simulation areas of size $L \times L$ containing N dislocations with Burgers vectors $\mathbf{b}_i = s_i(b, 0)$ where $s_i \in \{1, -1\}$ and $i \in [1..N]$. We assume equal numbers of dislocations of positive and negative signs. The CTD equations of motion read

$$\dot{x}_i = MF_i = Mbs_i \left[\sum_{j \neq i} s_j \sigma_{\text{ind}}(\mathbf{r}_i - \mathbf{r}_j) + \sigma_{\text{ext}} \right], \quad \dot{y}_i = 0. \quad (1)$$

Here M is the dislocation mobility, F_i the x component of the force per unit length acting on the i th dislocation, $\sigma_{\text{ind}}(\mathbf{r}) = Gb \cos(\phi) \cos(2\phi)r^{-1}$ is the shear stress field generated by an individual dislocation (with periodic boundary conditions assumed in both x and y directions, for details see [31]), G an appropriate elastic constant, and σ_{ext} is the external shear stress. The CA models are defined by discretizing the system both in space and time. Dislocations are allowed to move from one cell to a neighboring cell if such a move decreases the elastic energy of the system. We apply two different rules for the dynamics: (i) In extremal dynamics (ED) at each step only the move which produces the largest energy decrease is carried out. (ii) In random dynamics (RD) the moved dislocation is selected randomly from those that are allowed to move. The motivation of using all these models together is twofold: In the CA models it is easier to collect large amounts of statistics from larger systems, and the two CA dynamics correspond to highly non-linear relations between the acting force and the mean velocity of a dislocation. This makes it possible to test the generality of our results by comparing them with the linear force-velocity characteristics of the CTD model, Eq. (1). In what follows, we measure lengths, times and stresses in units of $\rho^{-0.5}$, $(\rho M G b^2)^{-1}$, and $G b \rho^{0.5}$, with $\rho = N/L^2$ the dislocation density [32]. As an example, it is noted that in these dimensionless units $N = L^2$.

A quasistatic stress-controlled loading protocol is implemented as follows. First, a random initial dislocation configuration is let to relax at $\sigma_{\text{ext}} = 0$ into a metastable arrangement. Then, for the continuous time model, σ_{ext} is increased at a slow rate from zero until the average dislocation velocity $V(t) = (1/N) \sum_i |\dot{x}_i(t)|$ exceeds a small threshold value V_{th} . While $V(t) > V_{\text{th}}$ and an avalanche propagates, the external stress is kept constant, and the amount of slip $s = \sum_i s_i \Delta x_i$ and plastic strain $\Delta \gamma = s/L^2$ produced within the avalanche are recorded. Here Δx_i denotes the displacement of the i th dislocation during the given avalanche. After the

avalanche is finished ($V(t) < V_{th}$), the external stress is again increased at a slow rate until the next avalanche is triggered. A similar loading protocol is implemented in the CA models: In between the avalanches, the external stress is increased just enough to make exactly one dislocation move, which then may trigger further dislocation activity, during which the applied stress is again kept constant.

For each model, we consider the avalanche size distribution $P(s)$ at different levels of the external stress below the yield stress. For $s > 1$ (i.e. slip events larger than that corresponding to a single dislocation moving one average dislocation spacing), these can be well characterized by a power law with a cut-off,

$$P(s) \propto s^{-\tau} f(s/s_0). \quad (2)$$

To estimate τ and s_0 , a fitting procedure has been used that fits Eq. (2) simultaneously to the avalanche distributions obtained at different stress levels and system sizes. The cutoff was found to follow

$$s_0(\sigma_{ext}, N) \propto N^\beta \exp(\sigma_{ext}/\sigma_0). \quad (3)$$

Table I compiles the parameters obtained by fitting Eqs. (2) and (3) to the avalanche size distributions. Fig. 2(a-c) shows the $P(s)$ distributions for the three models plotted as functions of s/s_0 . The validity of Eq. (3) is demonstrated by the collapse of all distributions in the cutoff region. Since Eq. (2) holds only for $s > 1$, the curves follow the master curve only as long as $s/s_0 > 1/s_0$, thus over longer range as the applied stress and/or the system size increase. Below this regime the behavior is governed by the single-dislocation dynamics and therefore differs between the three models.

The observations summarized by Eqs. (2), (3) and Table I exhibit several interesting features which are the main results of this Letter:

- (i) The power law exponent τ has the value $\tau \approx 1.0$, clearly different from the MFD value $\tau = 1.5$. According to Fig. 2(d), the integrated distribution (where avalanches with all stress values are considered together) exhibits a larger exponent $\tau_{int} \approx 1.3$, which is in line with a recent reanalysis of experimental micropillar compression data [33]. Moreover, Fig. 3 shows that in the CTD model, the avalanche size scales with the duration as $s \propto T^\gamma$, with $\gamma \approx 1.35$ clearly different from the MFD value of 2.
- (ii) According to Eq. (3), the cutoff s_0 increases with system size even at very small applied stress like $s_0 \propto N^\beta$ with $\beta \approx 0.4$.
- (iii) The cutoff s_0 does not diverge at a certain external stress, rather it exhibits an exponential stress dependence.

TABLE I. Parameters of Eqs. (2) and (3) obtained by fitting to the numerically obtained avalanche distributions.

Model	τ	β	σ_0
CTD	0.97 ± 0.03	0.36 ± 0.04	0.07 ± 0.01
CA with ED	1.00 ± 0.03	0.36 ± 0.02	0.116 ± 0.004
CA with RD	1.02 ± 0.01	0.44 ± 0.01	0.122 ± 0.002

The fundamental difference between the present and depinning behavior is highlighted in Fig. 1, where the average avalanche size is compared for a simple model showing depinning behavior and the CA DDD model with ED considered here.

Equation (3) implies that the cutoff of the plastic strain bursts $\Delta\gamma$ scales as $\Delta\gamma_0 = s_0/L^2 \propto N^{\beta-1} = L^{2\beta-2}$. Since $\beta < 1$, with increasing system size the observed plastic strain events get smaller, in line with the experimental evidence that macroscopic plasticity is a smooth process. We note that a similar scaling form (with $\beta \approx 0.5$) has been proposed for systems deforming in the strain hardening regime above the yield stress [2, 34]. The remarkable new finding here is that the same scaling holds also for very small stresses far below the yielding threshold. Furthermore, the energy dissipated during an avalanche (at a given external stress) scales as $E \propto \sigma_{ext} \Delta\gamma L^2 = \sigma_{ext} s$ [9], i.e. it diverges for large specimens at any applied stress. This is in accordance with AE results obtained during creep experiments on large ice single crystals which show that even for resolved shear stresses far below the yield stress, the energy releases recorded during AE events exhibit a power-law distribution which spans more than six orders of magnitude without any apparent cutoff [4, 5].

Thus, our results demonstrate that there are system size effects at every stress level. To understand the nature of these size effects we note that the spatial correlations of dislocation positions are short-ranged, with a correlation length ξ of the order of the average dislocation spacing $\xi \approx 0.25$ (in the scaled units introduced above) [35, 36] which defines the only internal length scale characterizing the dislocation structure. Given that the system sizes considered here are much larger, with L ranging from 44ξ ($N = 128$) to 256ξ ($N = 4096$), the size effect we observe is not related to this microscopic length scale. Therefore, we consider instead dynamic correlations in the motion of dislocations. To this end, we analyze the spatial structure of the avalanches in terms of the average spatial distribution of the plastic strain $\gamma(\mathbf{r})$ produced during an avalanche and its angular average $\gamma(r)$ (these quantities relates to the avalanche size by $s = \int \gamma(\mathbf{r}) d^2r = \int 2\pi r \gamma(r) dr$). To determine average values of these quantities, we shift the avalanche initiation points (taken to be the location of the fastest dislocation when V_{th} is exceeded) into the origin of a

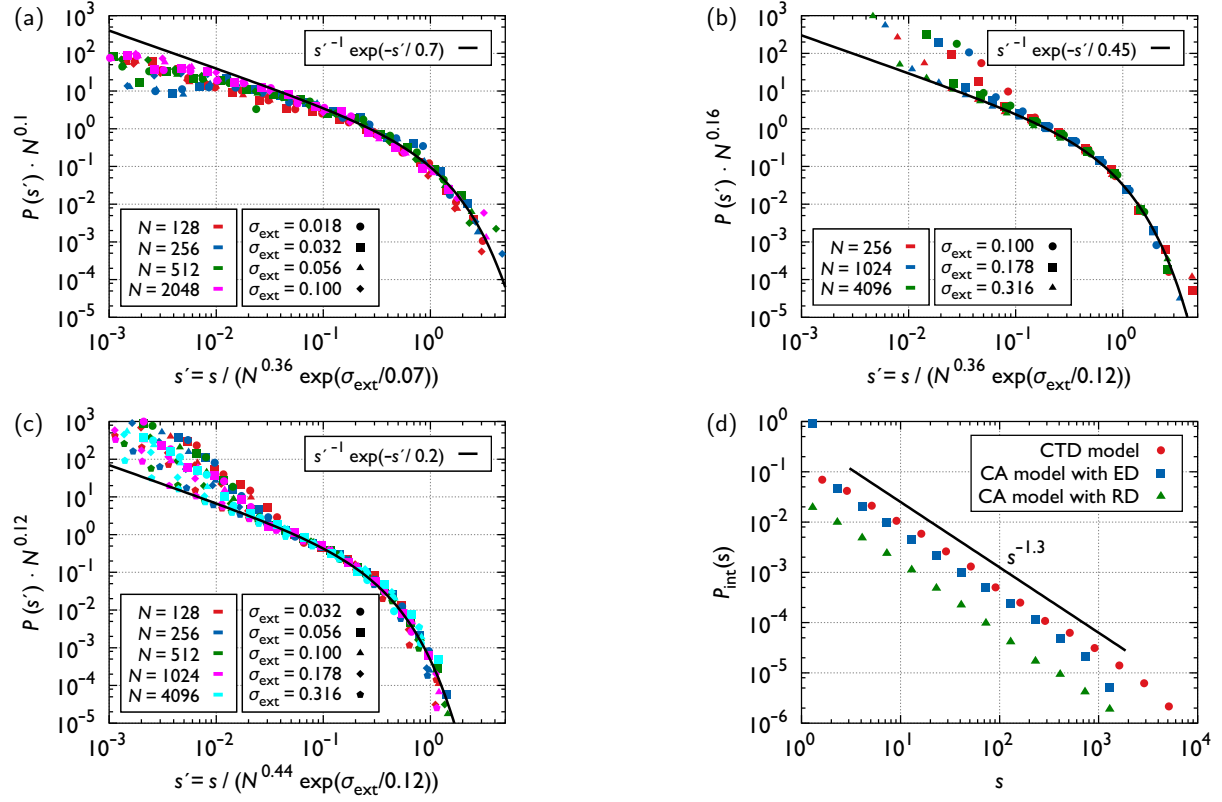


FIG. 2. (color online) (a-c) Stress-resolved distributions of avalanche sizes for the various DDD models at different applied stresses and system sizes. The distributions are plotted as functions of $s' := s/s_0$, with s_0 obeying Eq. (3). (a) CTD model, (b) CA model with ED, (c) CA model with RD. (d) Aggregate avalanche size distributions P_{int} integrated over σ_{ext} for system sizes $N = 512$ (CTD model) and $N = 4096$ (CA models).

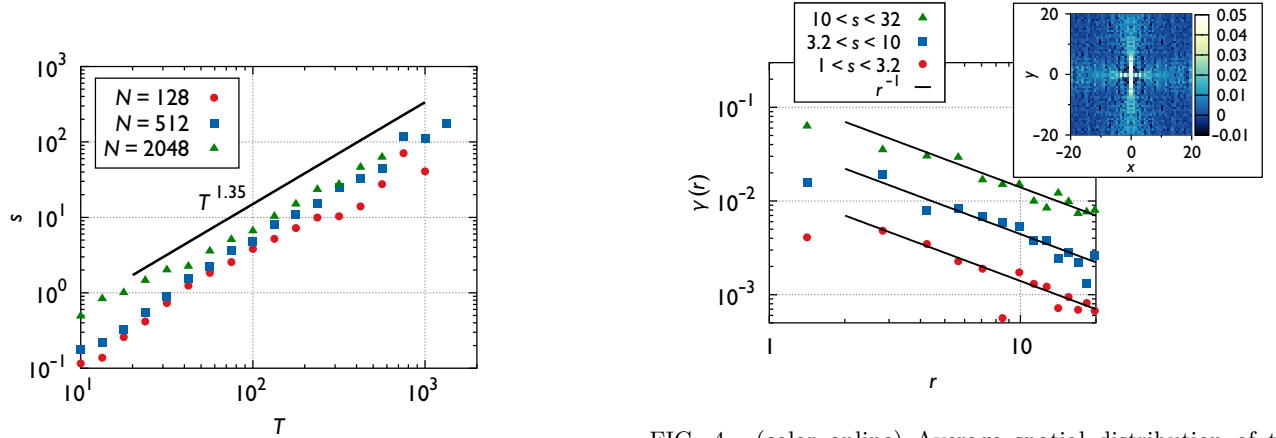


FIG. 3. (color online) Scaling of the avalanche size s with the duration T in the CTD model, for three different system sizes N . Notice how s for a given T increases with N .

Cartesian coordinate system and then average the superimposed strain patterns over multiple avalanches. Figure 4 demonstrates that $\gamma(\mathbf{r})$ exhibits a strongly anisotropic structure and decays slowly along the x and y axes. Averaged over all directions, the radial decay is of $1/r$ type

FIG. 4. (color online) Average spatial distribution of the avalanche plastic strain determined for avalanches occurring at $\sigma_{\text{ext}} \approx 0.08$ in the CTD model for $N = 2048$. Main figure: Radial decay of the angle-averaged plastic strain for avalanches of different sizes. Inset: Strain pattern $\gamma(\mathbf{r})$ averaged over all avalanches.

regardless of the avalanche size s . This indicates that the long-range stress fields of the moving dislocations are not fully screened (contrary to what is observed in equilibrium [36]), leading to highly non-local spreading of the

avalanche activity. Thus, even at low stresses avalanches are influenced by the finite system size, naturally leading to an L -dependent slip avalanche cutoff. The fact that this cutoff diverges with increasing L indicates that in the thermodynamic limit the system is scale-free in the dynamic sense even for small applied stresses. Analogous conclusions can be drawn from an investigation of the velocity distributions of dislocations during various relaxation scenarios [26] which demonstrates that the distributions follow at all stresses a simple scaling relation indicating the absence of a time-scale in the system.

To conclude, we have established that the statistics of slip avalanches in simple 2d DDD models is inconsistent with a depinning transition. Fundamental differences between the behavior of dislocation systems and the interface pinning/depinning scenario are manifested by the behavior of the cut-off of the avalanche size distribution which, rather than diverging at some critical stress σ_c , scales exponentially with stress but diverges with system size at every stress level. In addition, the avalanche exponent $\tau \approx 1.0$ is inconsistent with MFD. Rather than depinning, a possible analogy for the observed behavior is provided by avalanches in glassy systems, such as mean-field spin glasses [37, 38], where an exponent $\tau = 1$ and a size effect analogous to Eq. (3) have been observed. This is in line with other investigations which have shown that dislocation systems exhibit typical glassy properties such as slow relaxation [26, 32, 39] and aging [40].

While we have demonstrated that the equation "Yielding = Depinning" is not generally valid, it is important to note that real dislocation systems are composed of flexible lines moving in three dimensions and their behavior may differ from the present, highly idealized 2d models. Therefore, both 3d DDD simulation studies and experimental studies with large statistical samples are required in order to understand the stress-resolved statistics of dislocation avalanches in 3d and to settle the question regarding the fundamental nature of the yielding/jamming transition of dislocation systems.

Acknowledgments. This work has been supported by the Hungarian Scientific and Research Fund (P.D.I. and I.G., project nos. OTKA-PD-105256 and OTKA-K-105335); the European Commission (P.D.I., project no. MC-CIG-321842); and the Academy of Finland through a Postdoctoral Researcher's Project (L.L., project no. 139132), through an Academy Research Fellowship (L.L., project no. 268302), through the Centres of Excellence Program (project no. 251748), and via two travel grants (L.L., P.D.I., nos. 261262 and 261521). The numerical simulations presented above were partly performed using computer resources within the Aalto University School of Science "Science-IT" project. S.Z. is supported by the European Research Council, AdG2001-SIZEEFFECTS and thanks the visiting professor program of Aalto University.

-
- [1] D. M. Dimiduk, C. Woodward, R. LeSar, and M. D. Uchic, *Science* **312**, 1188 (2006).
 - [2] F. F. Csikor, C. Motz, D. Weygand, M. Zaiser, and S. Zapperi, *Science* **318**, 251 (2007).
 - [3] M. D. Uchic, P. A. Shade, and D. M. Dimiduk, *Annu. Rev. Mater. Res.* **39**, 361 (2009).
 - [4] J. Weiss and J.-R. Grasso, *J. Phys. Chem. B* **101** 6113 (1997).
 - [5] M.-C. Miguel, A. Vespignani, S. Zapperi, J. Weiss, and J. R. Grasso, *Nature* **410**, 667 (2001).
 - [6] D. S. Fisher, *Phys. Rep.* **301**, 113 (1998).
 - [7] S. Zapperi and M. Zaiser, *Mater. Sci. Engng. A* **309/310**, 348 (2001).
 - [8] B. Bakó, D. Weygand, M. Samaras, W. Hoffelner, and M. Zaiser, *Phys. Rev. B* **78**, 144104 (2008).
 - [9] M. Zaiser and P. Moretti, *J. Stat. Mech.* P08004 (2005).
 - [10] M. Zaiser, *Adv. Phys.* **54**, 185-245 (2006).
 - [11] K. A. Dahmen, Y. Ben-Zion, and J. T. Uhl, *Phys. Rev. Lett.* **102**, 175501 (2009).
 - [12] N. Friedman, A. T. Jennings, G. Tsekenis, J.-Y. Kim, M. Tao, J. T. Uhl, J. R. Greer, and K. A. Dahmen, *Phys. Rev. Lett.* **109**, 095507 (2012).
 - [13] P. M. Derlet and R. Maaß, *Modelling Simul. Mater. Sci. Eng.* **21**, 035007 (2013).
 - [14] G. Tsekenis, J. T. Uhl, N. Goldenfeld, and K. A. Dahmen, *EPL* **101**, 36003 (2013).
 - [15] K. S. Ng and A. H. W. Ngan, *Acta Mater.* **56**, 1712 (2008).
 - [16] S. Brinckmann, J.-Y. Kim, and J. R. Greer, *Phys. Rev. Lett.* **100**, 155502 (2008).
 - [17] M. Zaiser, J. Schwerdtfeger, A. S. Schneider, C. P. Frick, B. G. Clark, P. A. Gruber, and E. Arzt, *Philos. Mag.* **88**, 3861 (2008).
 - [18] D. Weygand, L. H. Friedman, E. Van der Giessen, and A. Needleman, *Model. Simul. Mater. Sc.* **10**, 437 (2002).
 - [19] R. Madec, B. Devincere, and L. P. Kubin, *Phys. Rev. Lett.* **89**, 255508 (2002).
 - [20] A. Arsenlis, W. Cai, M. Tang, M. Rhee, T. Oppelstrup, G. Hommes, T. G. Pierce, and V. V. Bulatov, *Mod. Simul. Mater. Sci. Eng.* **15**, 553 (2007).
 - [21] J. A. El-Awady, S. Bulent Biner, and N. M. Ghoniem, *J. Mech. Phys. Solids* **56**, 2019 (2008).
 - [22] M.-C. Miguel, A. Vespignani, M. Zaiser, and S. Zapperi, *Phys. Rev. Lett.* **89**, 165501 (2002).
 - [23] L. Laurson, M.-C. Miguel, and M. J. Alava, *Phys. Rev. Lett.* **105**, 015501 (2010).
 - [24] S. M. Keralavarma, T. Cagin, A. Arsenlis, and A. A. Benzerga, *Phys. Rev. Lett.*, **109**, 265504 (2012).
 - [25] V. V. Bulatov, L. L. Hsiung, M. Tang, A. Arsenlis, M. C. Bartelt, W. Cai, J. N. Florando, M. Hiratani, M. Rhee, G. Hommes, T. G. Pierce, and T. D. de la Rubia, *Nature* **440**, 1174 (2006).
 - [26] P. D. Ispánovity, I. Groma, G. Györgyi, P. Szabó, and W. Hoffelner, *Phys. Rev. Lett.* **107**, 085506 (2011).
 - [27] J. Rosti, J. Koivisto, L. Laurson, and M. J. Alava, *Phys. Rev. Lett.* **105**, 100601 (2010).
 - [28] P. Moretti, M.-C. Miguel, M. Zaiser, and S. Zapperi, *Phys. Rev. B* **69**, 214103 (2004).
 - [29] L. Laurson and M. J. Alava, *Phys. Rev. Lett.* **109**, 155504 (2012).
 - [30] G. Durin and S. Zapperi, *J. Stat. Mech.* P01002 (2006).

- [31] B. Bakó, I. Groma, G. Györgyi, and G. Zimányi, *Comp. Mater. Sci.* **38**, 22 (2006).
- [32] F. F. Csikor, M. Zaiser, P. D. Ispánovity, and I. Groma, *J. Stat. Mech.* P03036 (2009).
- [33] X. Zhang, B. Pan, and F. Shang, *EPL* **100**, 16005 (2012).
- [34] M. Zaiser and N. Nikitas, *J. Stat. Mech.* P04013 (2007).
- [35] M. Zaiser, M.-Carmen Miguel, and I. Groma, *Phys. Rev. B* **64**, 224102 (2001).
- [36] I. Groma, G. Györgyi, and B. Kocsis, *Phys. Rev. Lett.* **96**, 165503 (2006).
- [37] F. Pázmándi, G. Zaránd, and G. T. Zimányi, *Phys. Rev. Lett.* **83**, 1034 (1999).
- [38] P. Le Doussal, M. Müller, and K. J. Wiese, *EPL* **91**, 57004 (2010).
- [39] F. F. Csikor, B. Kocsis, B. Bakó, and I. Groma, *Mater. Sci. Eng. A* **400-401**, 214 (2005).
- [40] B. Bakó, I. Groma, G. Györgyi, G. T. Zimányi, *Phys. Rev. Lett.* **98**, 075701 (2007).